XXI IMEKO World Congress "Measurement in Research and Industry"
August 30 – September 4, 2015, Prague, Czech Republic

AXIAL HEAT TRANSFER EFFECTS ON THE PERFORMANCE OF A THERMAL DISPERSION MASS FLOW METER

Klemen Rupnik, *Jože Kutin*, *Ivan Bajsić*

Laboratory of Measurements in Process Engineering, Faculty of Mechanical Engineering, University of Ljubljana, Aškerčeva 6, SI-1000 Ljubljana, Slovenia, email: klemen.rupnik@fs.uni-lj.si

Abstract – The axial heat transfer effects on the performance of the thermal dispersion mass flow meter are studied by employing an analytical one-dimensional model and a numerical two-dimensional model of the thermal flow sensor. The relationship between the measurement characteristic and the temperature difference between the sensing element and the base is analysed and possible methods to practically implement the correction of the measurement characteristic are proposed.

Keywords: mass flow meter, thermal flow sensor, axial heat transfer effects, analytical approach, numerical simulation

1. INTRODUCTION

Thermal mass flow meters [1,2] are mostly used to measure the mass flow rate of gases. The measurement principle of the thermal dispersion mass flow meter is based on the heat transfer from the thermal flow sensor to the gas. The thermal flow sensor contains a resistance temperature sensing element that is heated in order to maintain a constant temperature difference above the gas temperature, where the heating electrical power changes with the mass flow rate. Another possibility is to maintain a constant electrical power, where the resulting temperature difference changes with the mass flow rate.

Heat transfer in the thermal flow sensor is influenced by its internal structure and thermal properties, and the process, installation and operation conditions. The basic measurement effect is related to the heat transfer from the sensing element to the gas. However, the axial heat transfer from the sensing element along the sensor's stem to the base may be also significant. Olin [3] presented a design of the thermal flow sensor comprising an additional temperature sensing element, which is used to evaluate the axial heat transfer rate. On the other hand, Pape and Hencken [4] modelled a similar thermal flow sensor with the purpose to analyse the effect of the coatings deposited on the surface of the thermal flow sensor on the measurement characteristic, which results from their influence on the axial heat transfer.

In this paper the effect of the axial heat transfer along the thermal flow sensor is studied employing a simple analytical one-dimensional model (Section 2) and a numerical two-dimensional model (Section 3). The latter takes into account more complex internal structure of the sensor and flow conditions, and both the convective and the radiative heat transfer from the sensor's surface. A correction of the measurement characteristic related to the axial heat transfer along the thermal flow sensor is proposed on the basis of the one-dimensional model and is validated by the results of the two-dimensional model (Section 4). This work complements our research and development of the thermal dispersion mass flow meter with the gas-identification capability [5–7].

2. THEORETICAL BACKGROUND

A simple physical model of the thermal flow sensor is presented in Fig. 1. The sensor is considered to consist of the sensing element and the upper and the lower stem. The sensor is exposed to the uniform gas flow with the mass flow rate q_m, which influences the convective heat transfer coefficient α. The sensing element is heated by means of the electrical power P for the constant temperature difference above the gas temperature $T_S = T_G + \Delta T$. At the location, where the sensor is inserted into the flow pipe (i.e., the base), the base temperature T_B is defined. The temperature difference between the sensing element and the base is $\Delta T_{SB} = T_S - T_B$. The radiative heat transfer is neglected.

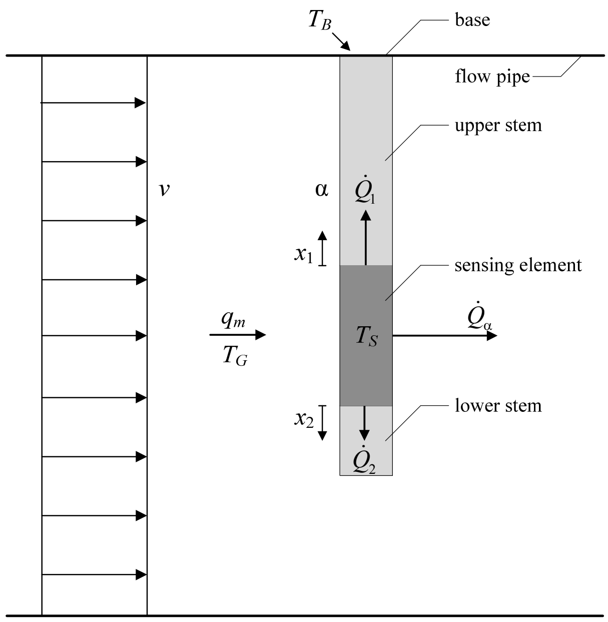

Fig. 1. Physical model of the thermal flow sensor exposed to the uniform gas flow.

The relationship between the supplied electrical power P and the mass flow rate q_m represents the measurement characteristic of the thermal flow sensor. The heat balance equation for the control volume defined with the sensing element is:

$$P = \dot{Q}_\alpha + \dot{Q}_1 + \dot{Q}_2 , \qquad (1)$$

where the convective heat transfer rate from the thermal flow sensor, having the area A of the outer surface, to the gas is:

$$\dot{Q}_\alpha = \alpha\, A\, \Delta T \qquad (2)$$

and the heat transfer rates from the sensing element to the upper and the lower stem are [8]:

$$\dot{Q}_1 = a_1\, b_1\, \Delta T\, \sqrt{\alpha}\, \frac{\cosh\left(b_1\sqrt{\alpha}\right) - 1 + \Delta T_{SB}/\Delta T}{\sinh\left(b_1\sqrt{\alpha}\right)} , \qquad (3)$$

$$\dot{Q}_2 = a_2\, b_2\, \Delta T\, \sqrt{\alpha}\, \frac{\sinh\left(b_2\sqrt{\alpha}\right) + c_2\sqrt{\alpha}\cosh\left(b_2\sqrt{\alpha}\right)}{\cosh\left(b_2\sqrt{\alpha}\right) + c_2\sqrt{\alpha}\sinh\left(b_2\sqrt{\alpha}\right)} , \qquad (4)$$

respectively, where $a_i = \lambda_i \pi d^2/(4L_i)$, $b_i = 2L_i(\lambda_i d)^{-1/2}$, $c_i = (d/(4\lambda_i))^{1/2}$, d is the diameter of the sensor, L_i is the length and λ_i is the thermal conductivity, where $i = 1$ denotes the upper stem and $i = 2$ denotes the lower stem. To obtain (3) and (4), the boundary conditions $T|_{x_1=L_1} = T_B$ and $\alpha\left(T|_{x_2=L_2} - T_G\right) = -\lambda_2\left(\mathrm{d}T/\mathrm{d}x\right)|_{x_2=L_2}$ were taken into account.

In the presented heat balance (1) only $\dot{Q}_1$ is influenced by ΔT_{SB}. This heat transfer rate can be written as:

$$\dot{Q}_1 = k\Delta T_{SB} + n\Delta T , \qquad (5)$$

where the constants are:

$$k = \frac{a_1\, b_1\sqrt{\alpha}}{\sinh\left(b_1\sqrt{\alpha}\right)}, \quad n = a_1\, b_1\sqrt{\alpha}\, \frac{\cosh\left(b_1\sqrt{\alpha}\right) - 1}{\sinh\left(b_1\sqrt{\alpha}\right)} . \qquad (6)$$

Consequently, the measurement characteristic for a given ΔT can be written as:

$$P = P_0 + k\Delta T_{SB} , \qquad (7)$$

where the component $P_0 = P_0(\alpha) = \dot{Q}_\alpha + n\Delta T + \dot{Q}_2$ is independent of ΔT_{SB} and can be determined as $P_0 = P|_{\Delta T_{SB}=0}$. The component $k\Delta T_{SB}$ is related to the axial heat transfer along the upper stem of the thermal flow sensor, where $k = k(\alpha)$ is the sensitivity coefficient that depends on the convective heat transfer coefficient $\alpha = \alpha(q_m)$ and consequently on the mass flow rate q_m. The sensitivity coefficient k is (in the non-dimensional form) presented in Fig. 2. Value of the sensitivity coefficient k decreases with the convective heat transfer coefficient α and consequently with the mass flow rate q_m.

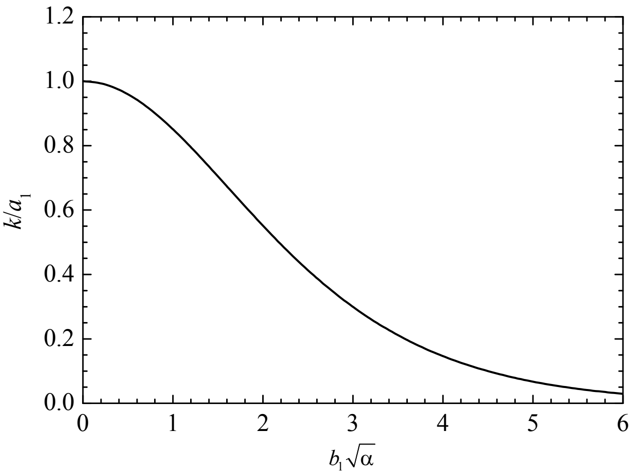

Fig. 2. Sensitivity coefficient k/a_1 of the axial heat transfer effect.

3. NUMERICAL MODEL

The computational domain of the numerical model of the thermal flow sensor is schematically presented in Fig. 3. Axisymmetric internal structure of the sensor with defined dimensions and thermal conductivities is taken into account. The thermal flow sensor is inserted into the flow pipe with the gas flow with defined pressure p, temperature T_G, mass flow rate q_m and velocity profile $v(x)$. Temperature of the internal surface of the flow pipe is T_p.

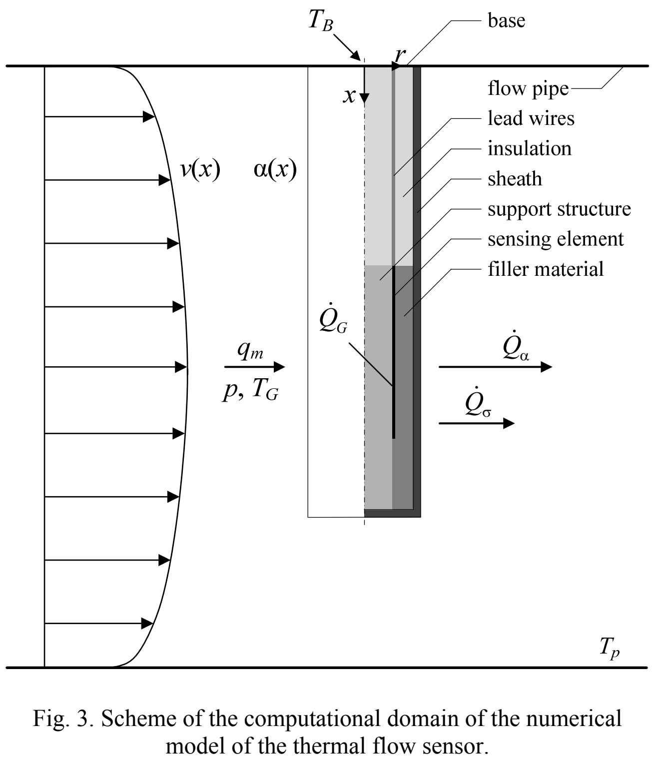

Fig. 3. Scheme of the computational domain of the numerical model of the thermal flow sensor.

The heat generation rate $\dot{Q}_G$ results from the electrical current I passing through the resistance temperature sensing element (equal to the heating electrical power P). The generated heat is conducted to the surface of the sensor, from where the convective and the radiative heat transfer take place, or conducted along the stem to the base.

The computational domain is discretized and for each computational cell the balance of heat generation rate and heat transfer rates across its boundaries is taken into account [9]. On the interfaces of the cells the internal boundary conditions based on heat conduction are taken into account. The following boundary conditions are considered on the external boundaries of the computational domain:

- axial symmetry of the sensor's internal structure,
- constant temperature at the upper boundary of the computational domain, which is equal to the base temperature T_B,
- convective heat transfer from the sensor's surface to the gas and radiative heat transfer from the sensor's surface to the internal surface of the flow pipe with considered temperature $T_p = T_G$.

The convective heat transfer coefficient is determined with the help of a semi-empirical model for convective heat transfer for a cylinder in the cross-flow, e.g., the Churchill-Bernstein model [10] is employed in this paper. The required thermodynamic and transport properties are determined using the NIST REFPROP database [11]. The gas velocity profile depends on the Reynolds number – for $\mathrm{Re}_D < 2000$ and $\mathrm{Re}_D > 4000$ the laminar and the turbulent velocity profiles, respectively, are taken into account [12].

With an additional equation the value of the average temperature of the sensing element is set as:

$$T_S = T_G + \Delta T\,. \tag{8}$$

The obtained system of equations is solved iteratively due to temperature-dependent coefficients. The values of the temperatures in the centres of the computational cells and the value of the electrical current are obtained as the solution of the system of equations, which enable us to calculate the heating electrical power P and the particular heat transfer rates, e.g., the convective and the radiative heat transfer rates, $\dot{Q}_\alpha$ and $\dot{Q}_\sigma$, respectively.

The numerical analyses employing the two-dimensional model were performed for the geometry of the computational domain that is based on the internal structure of a practical thermal flow sensor [7]. The thermal flow sensor with the diameter $d = 1.95$ mm is assumed to be inserted into the flow pipe with the internal diameter $D = 25$ mm. The insertion length is 21 mm. The computational domain is discretized into 1051 × 52 cells.

4. RESULTS

With the purpose to analyse the axial heat transfer effect on the performance of the thermal flow sensor, the simulations were performed for the gas temperature $T_G = 20$ °C, temperatures of the sensing element $T_S = 30 \ldots 40$ °C ($\Delta T = 10 \ldots 20$ K), base temperatures $T_B = 15 \ldots 40$ K and for the reference mass flow rates of air $q_{m,ref} = 1 \ldots 10000$ g/min. The range of mass flow rates corresponds to the typical Reynolds numbers Re_D for the thermal mass flow meters available on the market. With respect to Re_D, the laminar and the turbulent velocity profiles are taken into account for $q_{m,ref} < 43$ g/min and $q_{m,ref} > 86$ g/min, respectively. The simulations were not performed for the transitional region ($2000 \le \mathrm{Re}_D \le 4000$).

For each temperature difference ΔT, the value of the component $P_0/\Delta T$ was calculated by the numerical model using its definition in (7), with $\Delta T_{SB} = 0$ K taken into account. Fig. 4 shows the results for the selected case with $\Delta T = 10$ K. Values of $P_0/\Delta T$ vary for less than 0.51% for all discussed temperature differences $\Delta T = 10 \ldots 20$ K in the observed range of mass flow rates.

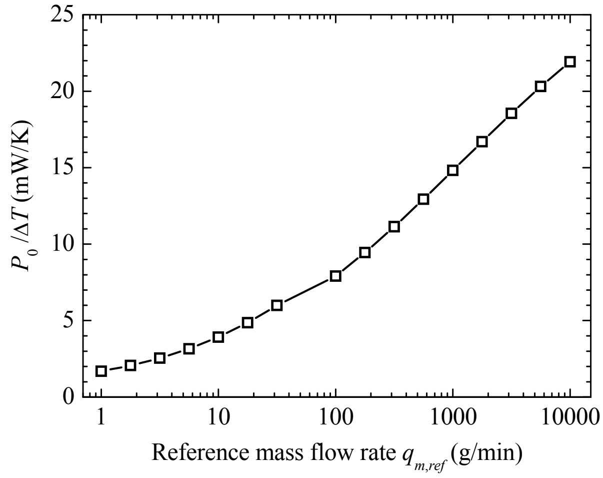

Fig. 4. Component $P_0/\Delta T$ for the selected temperature difference $\Delta T = 10$ K.

For each combination of the temperature differences ΔT and ΔT_{SB} (except for $\Delta T_{SB} = 0$ K), the sensitivity coefficient of the axial heat transfer effect was determined using (7) as:

$$k = \frac{P - P_0}{\Delta T_{SB}}\,. \tag{9}$$

Fig. 5 presents the sensitivity coefficient for the case with $T_G = 20$ °C, $T_S = 30$ °C ($\Delta T = 10$ K) and $T_B = 20$ °C ($\Delta T_{SB} = 10$ K). The sensitivity coefficient decreases with the mass flow rate, which is in agreement with the results of the

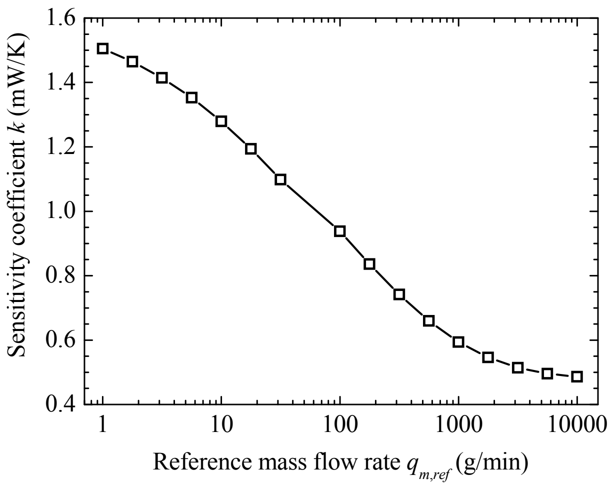

Fig. 5. Sensitivity coefficient k for the selected temperature differences $\Delta T = \Delta T_{SB} = 10$ K.

analytical one-dimensional model (Fig. 2). The portion of the component $k\Delta T_{SB}$ in the electrical power P is 47.1% at 1 g/min, and 2.2% at 10000 g/min, which shows that the axial heat transfer has larger relative effect on the measurement characteristic at lower mass flow rates.

With the purpose to estimate the variation of the sensitivity coefficient for different conditions, the relative difference is defined as:

$$e_r(k) = k / k_{\Delta T = \Delta T_{SB} = 10\ \mathrm{K}} - 1 \,. \quad (10)$$

If ΔT is constant and ΔT_{SB} varies, the absolute values of the relative differences are in the range of 0.035% despite large range of temperatures, which is presented in Fig. 6. Fig. 7 shows the relative differences for different values of ΔT and $\Delta T_{SB} = 10$ K. The absolute values of the relative differences are up to 0.45% (for $\Delta T = 20$ K) in the observed range of mass flow rates.

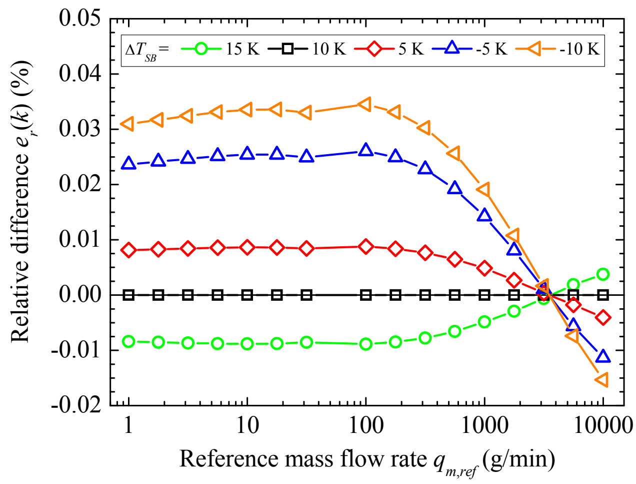

Fig. 6. Relative differences of the sensitivity coefficients for $\Delta T = 10$ K and different values of ΔT_{SB}.

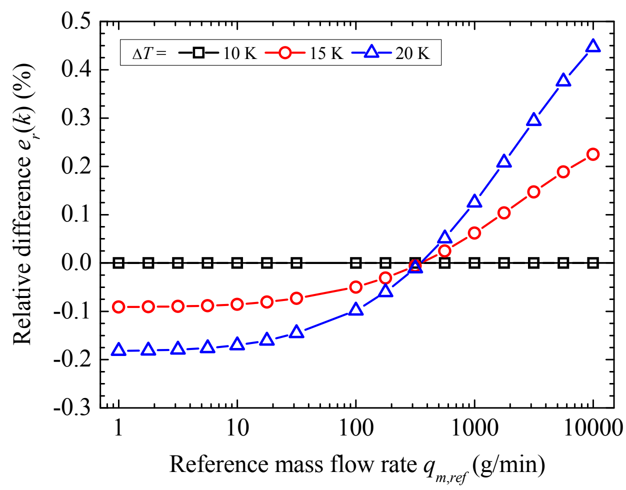

Fig. 7. Relative differences of the sensitivity coefficients for different values of ΔT and $\Delta T_{SB} = 10$ K.

Thermal mass flow meters typically operate at constant ΔT. The conditions at the installation location of the thermal mass flow meter can be different from the reference conditions at the calibration, e.g., the temperature of the ambient air affects the base temperature and consequently the axial heat transfer along the stem of the thermal flow sensor. The measurement characteristic without the correction of the axial heat transfer effect is described with the following measurement model:

$$P = \frac{1}{c_1 + \dfrac{1}{c_2 + c_3 q_m^{\,c_4}}} \Delta T \,, \quad (11)$$

where c_1, c_2, c_3 and c_4 are the calibration constants, which are determined by fitting the data sets of the electrical power P and the mass flow rate q_m. A disadvantage of this approach is that the calibration constants contain the effect of the axial heat transfer along the thermal flow sensor.

In addition to the uncorrected measurement characteristic, we will analyse the performance of the thermal flow sensor with the measurement characteristic with the correction of the axial heat transfer effect, which can be determined by employing (7):

$$P_0 = P - k\Delta T_{SB} \quad (12)$$

and fitted using the measurement model (11) to obtain the functional relationship $P_0 = P_0(q_m)$.

The numerical model was employed to simulate the discussed thermal flow sensor in the range of mass flow rates from 100 g/min to 1000 g/min for the following conditions: $T_G = 20$ °C, $T_S = 30$ °C ($\Delta T = 10$ K) and $T_B = 20$ °C ($\Delta T_{SB} = 10$ K). Both measurement characteristics, $P = P(q_m)$ and $P_0 = P_0(q_m)$, were determined based on this simulated calibration data. To obtain the latter, the sensitivity coefficient k for the given conditions from Fig. 5 was taken into account. The calibration constants, obtained by the Levenberg-Marquardt curve-fitting method, are presented in Table 1.

Table 1. Calibration constants of the measurement model (11) with P (mW) or P_0 (mW) and q_m (g/min), for $\Delta T = 10$ K and $q_m = 100 \ldots 1000$ g/min.

	$c_1 \times 10^3$	c_2	$c_3 \times 10^3$	c_4
$P(q_m)$	32.21	1.845	1.413	0.436
$P_0(q_m)$	32.85	–0.0265	1.474	0.431

The validation of the proposed correction method was carried out in order to evaluate the performance of the correction of the axial heat transfer effect, which was simulated by changing the base temperature T_B to 19.5 °C ($\Delta T_{SB} = 10.5$ K) and 20.5 °C ($\Delta T_{SB} = 9.5$ K). The mass flow readings q_m were determined employing both measurement characteristics and then the relative errors with respect to the reference mass flow rates $q_{m,ref}$ were calculated as:

$$e_r(q_m) = q_m / q_{m,ref} - 1 \,. \quad (13)$$

The relative errors for the measurement characteristic without the correction of the axial heat transfer effect are presented in Fig. 8. If the considered conditions are different from the reference conditions, the absolute values of the relative errors are up to 2% at lower mass flow rates and decrease with the mass flow rate. Therefore, the axial heat transfer has smaller relative effect at higher values of the mass flow rates. If the uncorrected measurement characteristic is used at reference conditions, the relative errors are up to 0.01%, which result from the estimation error of fitting the measurement characteristic. Fig. 8 also shows the results for the uncorrected measurement characteristic corresponding to $\Delta T = 20$ K, while the other conditions are the same as considered in the previous case. The relative errors are approximately two times smaller in comparison with those for $\Delta T = 10$ K, which indicate that the relative effect of the change of the base temperature is smaller at larger temperature difference ΔT.

The relative errors for the measurement characteristics with the correction of the axial heat transfer effect are shown in Fig 9. Even though the base temperature was changed, the

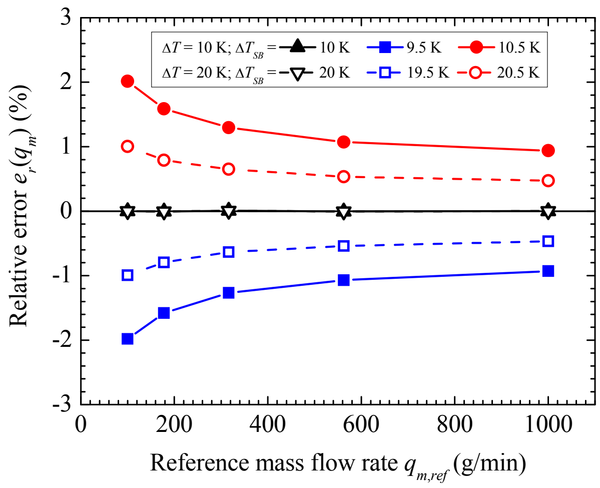

Fig. 8. Relative errors of the mass flow readings for the measurement characteristics without the correction of the axial heat transfer effect.

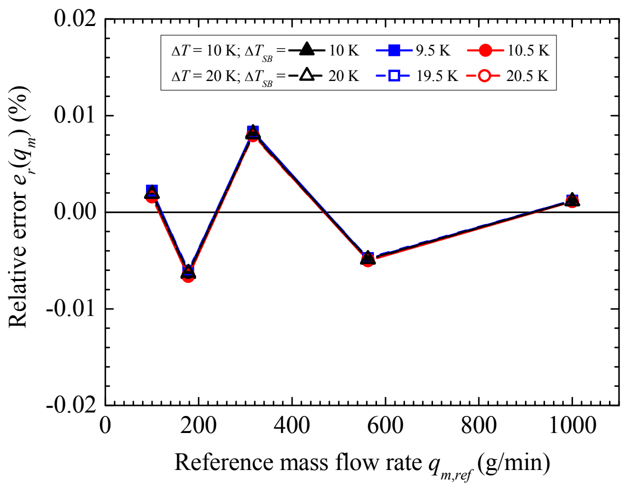

Fig. 9. Relative errors of the mass flow readings for the measurement characteristics with the correction of the axial heat transfer effect.

absolute values of the relative errors are less than 0.01%. Therefore, the axial heat transfer effect was successfully corrected. The correction works well also at lower mass flow rates, where the axial heat transfer has larger relative effect.

5. CONCLUSIONS

The axial heat transfer effect on the measurement characteristic of the thermal dispersion mass flow meter was studied by employing the analytical one-dimensional model. It was derived that the measurement characteristic is linearly dependent on the temperature difference between the sensing element and the base. This relationship was also validated by employing the two-dimensional numerical model that takes into account more complex internal structure of the sensor and flow conditions, and both the convective and the radiative heat transfer from the sensor's surface.

To practically implement the proposed method for the correction of the measurement characteristic, the thermal flow sensor should contain an additional temperature sensing element with the purpose to measure the base temperature. Even if both the temperature difference ΔT and the gas temperature T_G are constant, the base temperature T_B will generally vary with mass flow rate, because it is affected by the axial heat transfer along the thermal flow sensor. A possible way to experimentally determine the sensitivity coefficient k is presented below. The thermal flow sensor is calibrated for two temperature differences ΔT_1 and ΔT_2 in order to obtain two measurement characteristics (written in the form of $P/\Delta T$):

$$\frac{P_1}{\Delta T_1} = \frac{P_{0,1}}{\Delta T_1} + k\frac{\Delta T_{SB,1}}{\Delta T_1}, \tag{14}$$

$$\frac{P_2}{\Delta T_2} = \frac{P_{0,2}}{\Delta T_2} + k\frac{\Delta T_{SB,2}}{\Delta T_2}. \tag{15}$$

If we assume that components $P_{0,1}/\Delta T_1$ and $P_{0,2}/\Delta T_2$ are equal, the sensitivity coefficient can be calculated as:

$$k = \frac{P_2/\Delta T_2 - P_1/\Delta T_1}{\Delta T_{SB,2}/\Delta T_2 - \Delta T_{SB,1}/\Delta T_1}. \tag{16}$$

Because ΔT affects $P_0/\Delta T$ (see the discussion in Section 4), the difference between ΔT_1 and ΔT_2 should not be large in order to fulfil $P_{0,1}/\Delta T_1 \approx P_{0,2}/\Delta T_2$. On the other hand, the conditions of such calibration should assure that the denominator of (16) does not limit to zero.

An alternative solution to implement the correction of the axial heat transfer effect is that the additional temperature sensing element is not only used to measure the base temperature, but also employed as a heater to maintain a constant temperature difference between the base and the gas $T_B - T_G$. In the case of $\Delta T_{SB} = 0$ K, the mass flow readings would not be affected by the axial heat transfer. However, it would be reasonable to maintain a smaller temperature difference $T_B - T_G$ in comparison with the temperature difference ΔT (e.g., due to lower energy consumption for heating the base), which results in

$\Delta T_{SB} > 0$ K. In such case, the correction method could be performed as presented in Section 4.

ACKNOWLEDGMENTS

This work was supported in part by the Slovenian Research Agency.

REFERENCES

[1] R. C. Baker, *Flow Measurement Handbook: Industrial Designs, Operating Principles, Performance, and Applications*, Cambridge University Press, New York, 2000.

[2] *ISO 14511: Measurement of Fluid Flow in Closed Conduits – Thermal Mass Flowmeters*, International Standardization Organization, Geneva, 2001.

[3] J. G. Olin, *Mass Flow Meter System for Multi-Fluid Use without Fluid-Specific Calibration*, patent application WO2014046675, 2014.

[4] D. Pape and K. Hencken, "Dual sensor setup for thermal mass flow sensor diagnostics", *16. GMA/ITG-Fachtagung Sensoren und Messsysteme 2012*, pp. 282-290, Nürnberg, Germany, May 2012.

[5] K. Rupnik, J. Kutin and I. Bajsić, "A method for gas identification in thermal dispersion mass flow meters", *Strojniški vestnik – Journal of Mechanical Engineering*, vol. 60, n^o. 9, pp. 607-616, Sept. 2014.

[6] K. Rupnik, J. Kutin and I. Bajsić, *Thermal Mass Flow Meter and the Gas-Identification Method*, patent application WO2015088452, 2015.

[7] K. Rupnik, *Development of Thermal Mass Flow Meter*, Ph.D. Thesis, University of Ljubljana, Faculty of Mechanical Engineering, Ljubljana, 2014 (in Slovene).

[8] F. P. Incropera, D. P. DeWitt, T. L. Bergman and A. S. Lavine, *Fundamentals of Heat and Mass Transfer*, *6th edition*, John Wiley & Sons, Hoboken, 2007.

[9] J. R. Welty, *Engineering Heat Transfer*, John Wiley & Sons, New York, 1974.

[10] S. W. Churchill and M. Bernstein, "A correlating equation for forced convection from gases and liquids to a circular cylinder in crossflow", *Journal of Heat Transfer*, vol. 99, n^o. 2, pp. 300-306, May 1977.

[11] E. W. Lemmon, M. L. Huber and M. O. McLinden, *REFPROP: Reference Fluid Thermodynamic and Transport Properties, NIST Standard Reference Database 23, Version 9.0*, National Institute of Standards and Technology, Gaithersburg, 2010.

[12] R. D. Blevins, *Applied Fluid Dynamics Handbook*, Krieger Publishing Company, Malabar, 1992.